ELSEVIER

Palaeogeography, Palaeoclimatology, Palaeoecology 201 (2003) 269–281

PALAEO

www.elsevier.com/locate/palaeo

No aridity in Sunda Land during the Last Glaciation: Evidence from molecular-isotopic stratigraphy of long-chain *n*-alkanes

Jianfang Hu [a,*], Ping'an Peng [a], Dianyong Fang [b], Guodong Jia [a], Zhimin Jian [b], Pinxian Wang [b]

[a] *State Key Laboratory of Organic Geochemistry, Guangzhou Institute of Geochemistry, Chinese Academy of Sciences, Guangzhou 510640, PR China*

[b] *Laboratory of Marine Geology, Tongji University, Shanghai 200092, PR China*

Received 4 February 2002; received in revised form 22 July 2003; accepted 11 August 2003

Abstract

Molecular distribution and stable carbon-isotopic composition ($\delta^{13}C$) of *n*-alkanes determined in a sediment core (17962) from the southern South China Sea (SCS) show that no obvious change has taken place in vegetation on Sunda Land from the last glacial period to the beginning of the Holocene. A shift in the accumulation rate of long-chain *n*-alkanes (C_{27} to C_{33}) was recorded at a depth of about 620 cm, probably indicative of precipitation enhancement related to winter monsoon. The $\delta^{13}C$ values are within the range of −33.7 to −27.1‰ for C_{29} *n*-alkanes and −33.9 to −28.4 for C_{31} *n*-alkanes in the whole core sequence. Such an isotopic composition is characteristic of *n*-alkanes biosynthesized mainly by plants utilizing the C_3 photosynthetic pathway. Continuous development of C_3 plants on Sunda Land and its surroundings evidences that the climate during the last glacial period in the southern SCS was not drier than what it is today.

Keywords: South China Sea; long-chain *n*-alkanes; carbon-isotopic composition; aridity; Late Quaternary

1. Introduction

The stable carbon-isotopic composition ($\delta^{13}C$) of sedimentary organic matter has been used to identify organic material derived from land plants using different metabolic pathways (Huang et al., 1995; Huang et al., 2000; Huang et al., 2001). Stable carbon-isotopic analyses of total leaf tissues from plants utilizing different pathways of carbon fixation have shown that the plants which employ the Calvin cycle pathways (C_3 plants) during photosynthesis are more depleted in ^{13}C than plants which use the Hatch–Slack pathway (C_4 plants)(Smith and Epstein, 1971; Collister et al., 1994). Changes in $\delta^{13}C$ values of organic matter in sediments derived from the plants are partly

* Corresponding author. Tel.: +86-20-85290186; Fax: +86-20-85290117.

E-mail addresses: hujf@gig.ac.cn (J. Hu), pinganp@gig.ac.cn (P. Peng).

0031-0182/03/$ – see front matter © 2003 Elsevier B.V. All rights reserved.
doi:10.1016/S0031-0182(03)00613-8

attributed to climate-induced variations such as atmospheric pCO_2 (Kuypers et al., 1999), aridity (Sukumar et al., 1993) and temperature (Pagani et al., 1999). Huang et al. (2001) found that greater C_4 plant abundance only occurred when low pCO_2 coincided with increased aridity and that low pCO_2 alone was insufficient to trigger the expansion of C_4 plants in the absence of favorable climatic conditions.

The South China Sea (SCS) is located between the Asia landmass and the West Pacific and is one of the largest marginal seas in the world (Wang and Wang, 1990). In the southern SCS, a vast area, Sunda Land, emerged during glacial times owing to low sea level (Gupta et al., 1987; Pelejero et al., 1999a,b; Fig. 1) and the Molengraaff River was developed in this emergent tropical lowland (Molengraaff, 1921). Because of its location, the sediment sequence recorded in the SCS is affected by both the ocean and continent, thus recording both the history of continental climatic change and paleoceanographic change.

The East Asian Monsoon played an important role in the climate fluctuation of the SCS. The pollen record from Core 17940 shows that the climate was drier in the northern slope of the SCS at the last glaciation (Sun and Li, 1999). At the same time, the noticeable discharge of loess dust and markedly lowered sea-surface temperature (SST) during winter indicate that the winter monsoon strongly intensified and the summer monsoon weakened during the last glacial stage (Wang and Wang, 1990), which strongly reduced summer monsoon precipitation in the northern continental shelf of the SCS (Wang et al., 1999). All evidence suggests that in the northern SCS the climate was drier during the last glacial period.

However, whether the paleoclimate was dry or not in the southern continental shelf of the SCS during the last glacial period has been a long-standing controversy. Broecker et al. (1988) found that an abrupt decrease in sedimentation rate occurred from glacial time to Holocene in the southern SCS (Core V35-5; Fig. 1) and ascribed the higher glacial erosion rates during the glacial periods to drier climatic conditions which had prevailed in the Southeast Asia region, hence reducing the vegetation cover (savanna rather than rainforest). Moreover, van der Kaars et al. (2000) revealed that cooler and drier climatic conditions prevailed in the Indonesian region during the glacial periods and suggested that the reduction in humidity was due to the emergence of the Sunda Shelf, causing moisture availability at lower altitudes to reduce. Kershaw et al. (2002) also concluded that the precipitation decreased during glacial times in the Indonesian/northern Australian region based on pollen analysis. All these conclusions disagreed with the studies by Sun et al. (2000), who mapped the paleovegetation on the Sunda Shelf (Fig. 1). Moreover, the $\delta^{18}O$ and $\delta^{13}C$ values of planktonic foraminifera *Globigerinoides ruber* (Wang et al., 1999), and the concentrations of C_{37} alkenones, *n*-nonacosane and *n*-hesacosan-1-ol reflected that multi-episodic extreme precipitation occurred in the southern SCS during the last climate cycle (Pelejero et al., 1999a,b).

The present work is focused on molecular and compound-specific isotopic analyses of *n*-alkanes extracted from southern SCS sediments and provides new evidence for paleovegetation and paleoclimate changes on the Sunda Shelf of the southern SCS.

2. Samples and methods

2.1. Sediment samples

The sediment samples used in this study were taken from Core 17962 (Fig. 1) under the 'Monitor Monsoon' Project during the R/V *Sonne* Cruise 95 in April–June 1994 (Sarnthein et al., 1994). Core 17962 (7°11′N, 112°5′E) was obtained from a submerged central reef platform in the southern SCS, northwest of Borneo at a water depth of 1968 m, and in front of the 'Molengraaff River', which debouched from the Sunda Shelf during glacial times (Molengraaff, 1921; Fig. 1). Sediments were subsampled at 2.5 cm intervals over the whole core length, 800 cm. The core sequence is composed of calcareous pelitic/silty clays and is uniform with no sign of being disturbed.

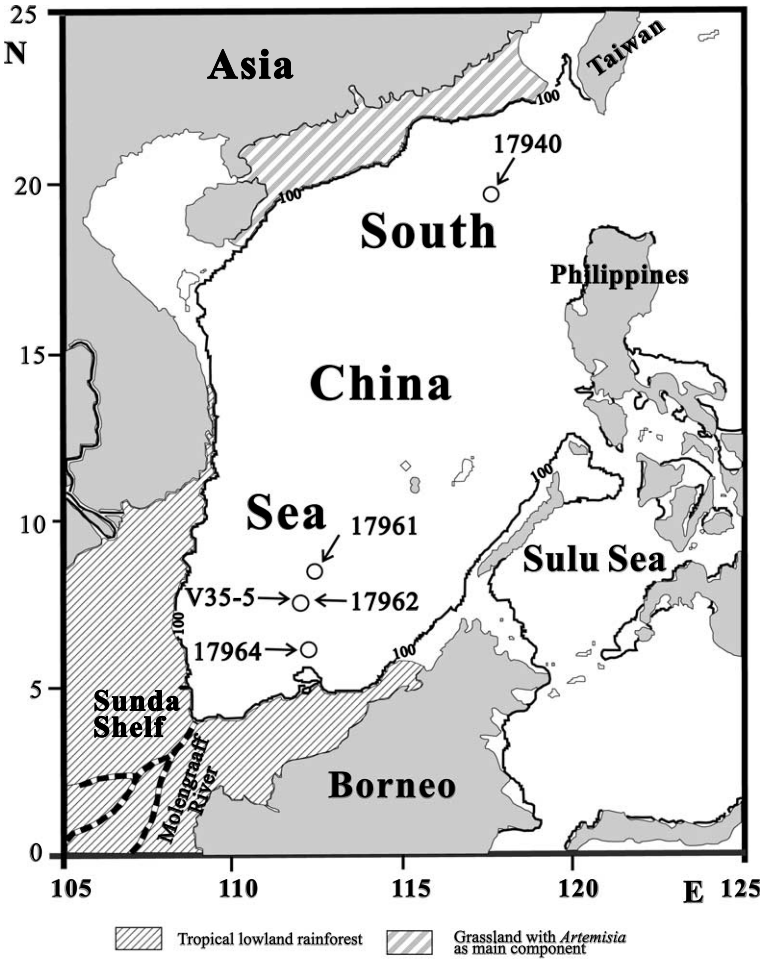

Fig. 1. Core 17962 sample localities in the SCS and sketch of vegetation reconstruction for the exposed shelves of the low-latitude West Pacific during the LGM from Sun et al. (2000). Present 100-m isobath shows the approximate position of the coastline during glacial low sea level (Wang et al., 1999).

2.2. Age model

The age model of Core 17962 was obtained by comparing it in detail with Core V35-5 (7°12′N, 112°5′E; Fig. 1) in terms of the concentrations of carbonate, the relative abundance of planktonic foraminiferal species (Fig. 2), and planktonic foraminiferal oxygen and carbon-isotope stratigraphy data (D. Fang, personal communication, 2001). As shown in Fig. 2, the concentrations of carbonate and the relative abundance of planktonic foraminiferal species in Cores 17962 and V35-5 are comparable. The chronology for Core V35-5 was documented by radiocarbon measurements by accelerator mass spectrometry (AMS) on planktonic shells of the species *Globigerinoides sacculifera* and *Pulleniatina obliquiloculata* (Broecker et al., 1988). However, the AMS ^{14}C ages obtained from planktonic foraminifera *G. sacculifera* and *P. obliquiloculata* are not consistent with each other. For example, at the depth of 175 cm, their ages are 12.2 kyr BP and 13.5 kyr BP, respectively. As it is difficult to interpret the difference and to determine which one is more accurate, the dating is open to objection (Broecker et al., 1988). In this study, AMS ^{14}C ages of

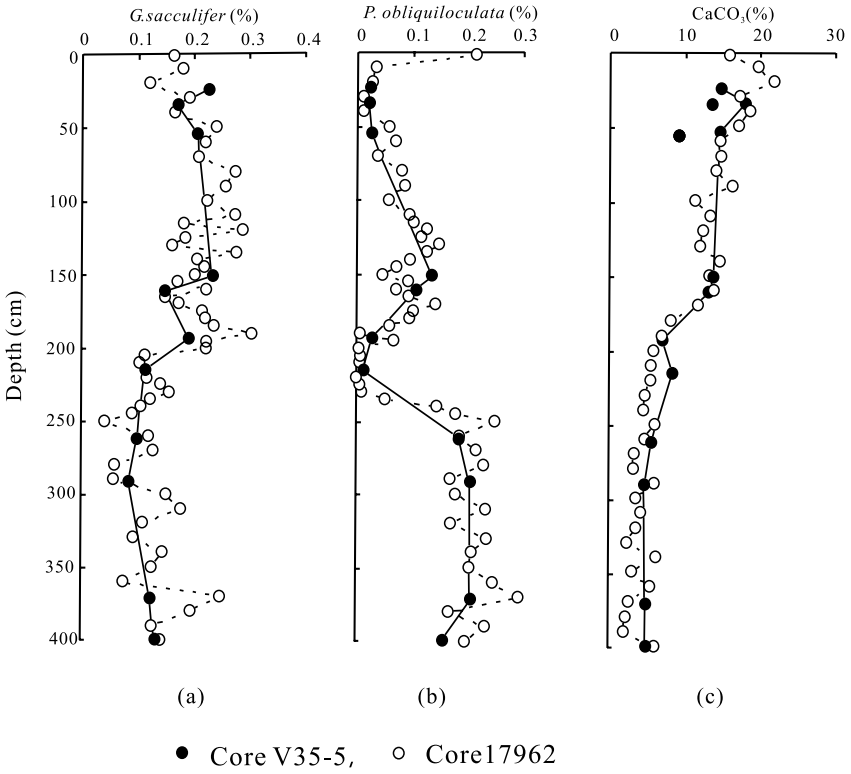

Fig. 2. Comparison of the percentages of planktonic foraminifera and carbonate contents for Cores 17962 and V35-5.

G. sacculifera were adopted, and calibrated for calendar years using University of Washington Quaternary Isotopelab Radiocarbon Calibration Program Rev. 3.03 by L. Wang at Kiel University. 400 yr was taken into account for calibration of the reservoir age of seawater. Broecker et al. (1988) marked the boundary between the last glaciation and the Holocene at the 175 cm level in Core V35-5, and this level is quoted for Core 17962 in this paper. Table 1 shows the main age information about Core 17962.

2.3. Analytical methods

Organic lipids were extracted from the homogenized wet sediments with the suspension of each of the samples using the following solvents: twice with methanol, once with a mixture of methanol and chloroform (1:1, v/v), and finally twice with chloroform. The suspension was made by mixing approximately 1 g of each sample with 8 ml of solvent, followed by stirring for 6 h. The resulting mixture was centrifuged and the supernatant solution was taken and transferred to a round-bottom flask. Known amounts of internal standards – palmatic acid-d_{31} and *n*-tetracosane-d_{50} ($C_{24}D_{50}$) – were added to the sample after the second extraction with methanol for quantification of molecular compounds. Then, the organic phase was separated from the aqueous phase after the addition of 15 ml of 0.1 M KCl solution by means of a separation funnel. The aqueous layer was extracted with chloroform (2×15 ml) and the collected organic phase was dried with anhydrous sodium sulfate overnight. After filtration, the organic solution was concentrated by way of rotary evaporation to 0.5 ml and then transferred to a 2 ml vial. After evaporation under nitrogen, the resulting extract was derivatized with *bis*-trimethylsilyl-trifluoroacetamide (BSTFA) and pyridine for gas chromatograph-mass spectrometer (GC/MS) analysis.

In order to obtain the QA/QC (quality assurance/quality control) indices for the method, two

Table 1
AMS ^{14}C ages dated on Core 17962

Sample depth (cm c.d.)	Planktonic foraminifera species	AMS ^{14}C age[a] (yr BP)	Calibrated age[b] (yr BP)	Error σ (yr)
10	*G. sacculifer*	1 870	1 390	± 150
5	*G. sacculifer*	2 055	1 603	± 100
64.5	*G. sacculifer*	5 750	6 171	± 120
82.5	*G. sacculifer*	7 670	8 077	± 140
102.5	*G. sacculifer*	9 050	9 660	± 130
127.5	*G. sacculifer*	9 910	10 823	
142.5	*G. sacculifer*	11 300	12 823	± 120
187.5	*G. sacculifer*	13 230	15 162	± 190
215	*G. sacculifer*	13 740	15 943	± 190
309.25	*G. sacculifer*	16 960	19 584	± 260

[a] AMS ^{14}C ages of *G. sacculifer* measured on Core V35-5 (Broecker et al., 1988).
[b] Calibrated ages which are calculated from AMS ^{14}C ages of Core V35-5 using University of Washington Quaternary Isotopelab Radiocarbon Calibration Program Rev. 3.03 by L. Wang. Reservoir age: 400 yr.

kinds of experiment were performed beforehand. First, in the experiment with standards added in the blank sample, run as done by the above analytical methods, the recoveries of tetracosane-d_{50}, palmitic acid-d_{31}, cholesterol and 1-hexacosanol are 95.8 ± 2.9%, 92.3 ± 2.3%, 99.7 ± 2.3% and 93.7 ± 1.6%, respectively. Second, in the experiment with standards added in the mineral matrix, the recoveries of tetracosane-d_{50}, palmitic acid-d_{31}, cholesterol and 1-hexacosanol are 94.8 ± 3.9%, 90.8 ± 4.5%, 98.8 ± 3.9% and 92.54.1% respectively. These data show that the analytical method is reliable.

To monitor the quality of each batch run of the experiments, a parallel blank sample with standards added was tested. The standards are tetracosane-d_{50}, 1-hexacosanol, palmitic acid-d_{31} and cholesterol and their recoveries are under the control of QA/QC.

The concentrations of *n*-alkane homologs were calculated by comparing the peak area of the appropriate compound to that of the internal standard – deuterated *n*-alkane $C_{24}D_{50}$ under the GC/MS chromatogram at *m/z* 85 and 99.

Analyses were carried out on a Finnigan GC 8000-Voyager GC/MS equipped with an on-column injector and a fused silica capillary column (Chrompack, 50 m × 0.32 mm, film thickness 0.25 μm). Helium was used as the carrier gas. The temperature programming was 45°C for 2 min, 45–120°C at 10°C/min, 120–300°C at 4°C/min and then isothermal for 30 min. The EI model with an energy source of 70 eV was adopted in the mass spectrometer.

The analyzed extracts were then evaporated till dryness under N_2 stream after GC/MS analysis. The residue was dissolved in *n*-hexane and the compounds were separated by column chromatography using 2 g silica gel; hydrocarbons were eluted with 10 ml *n*-hexane. The hydrocarbon fractions obtained by these procedures were concentrated to 0.2 ml and then analyzed for the carbon-isotopic composition of individual *n*-alkanes.

The carbon-isotopic values of individual *n*-alkanes were determined using a gas chromatography-isotope ratio mass spectrometry (GC-IRMS) system. A Hewlett-Packard 6890 gas chromatograph was used, equipped with an on-column injector, and interfaced with a Finnigan DELTA plus XL mass spectrometer via a combustion oven (940 °C). The *n*-alkanes were separated on a DB-5 fused silica capillary column (30 m × 0.32 mm i.d.; 0.25 μm film thickness). Helium was used as the carrier gas. The GC oven temperature was programmed from 55 to 210°C at 15°C/min for 2 min, from 210 to 290°C at 3°C/min, and then isothermal for 20 min. Pre-isotopic calibrated CO_2 was used as the standard. All $\delta^{13}C$ values are the average of two or three measurements ($\sigma = \pm 0.5$‰) and expressed as ‰ relative to the PeeDee Belemnite (PDB) standard.

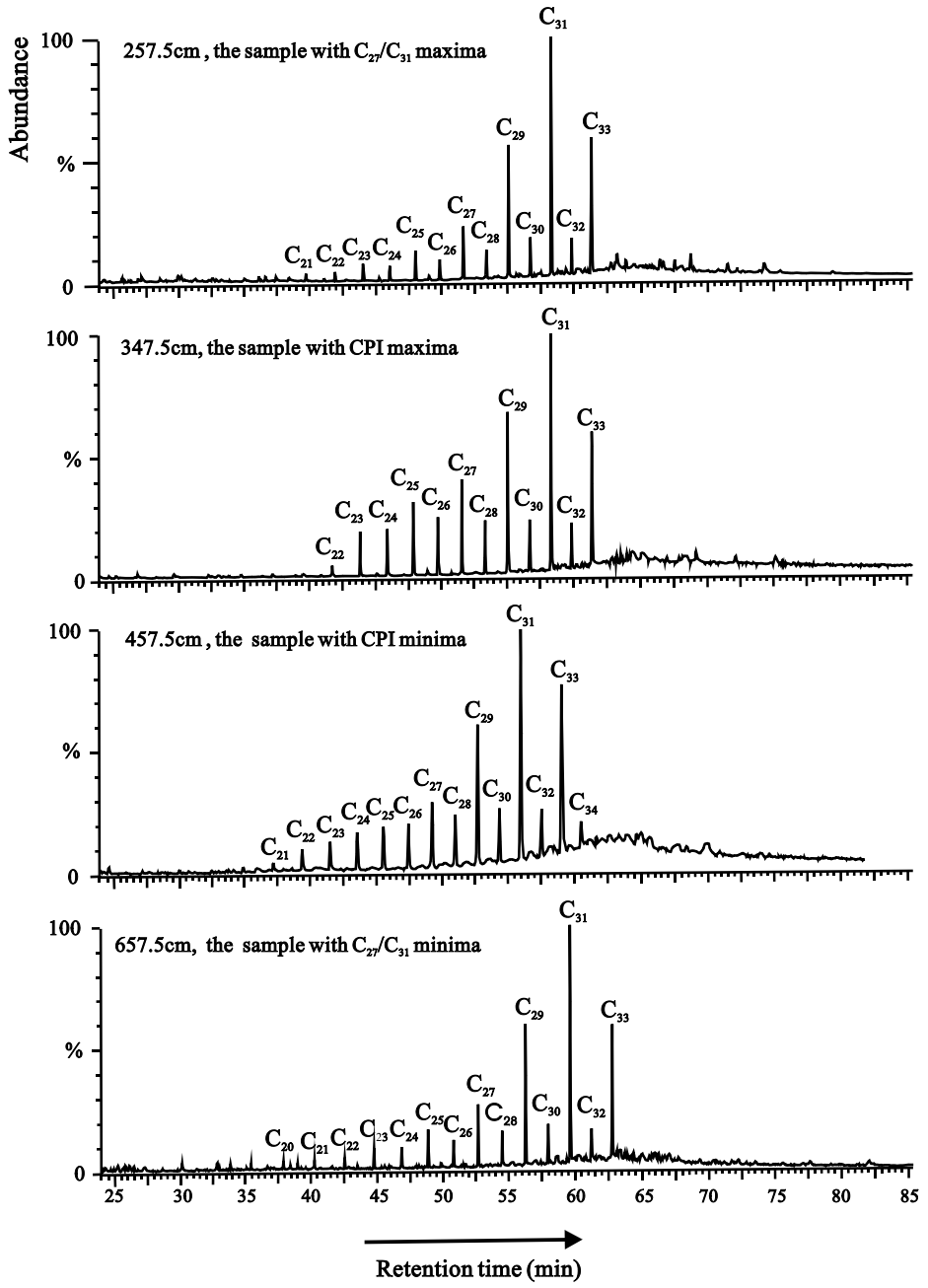

Fig. 3. *m/z* 85 Mass chromatograms showing *n*-alkanes are hydrocarbon fractions from the selected sediment samples from Core 17962. Numbers above the peaks stand for carbon chain lengths. Samples were selected to display the extremes of distributions viz. low and high CPI and high and low C_{27}/C_{31}.

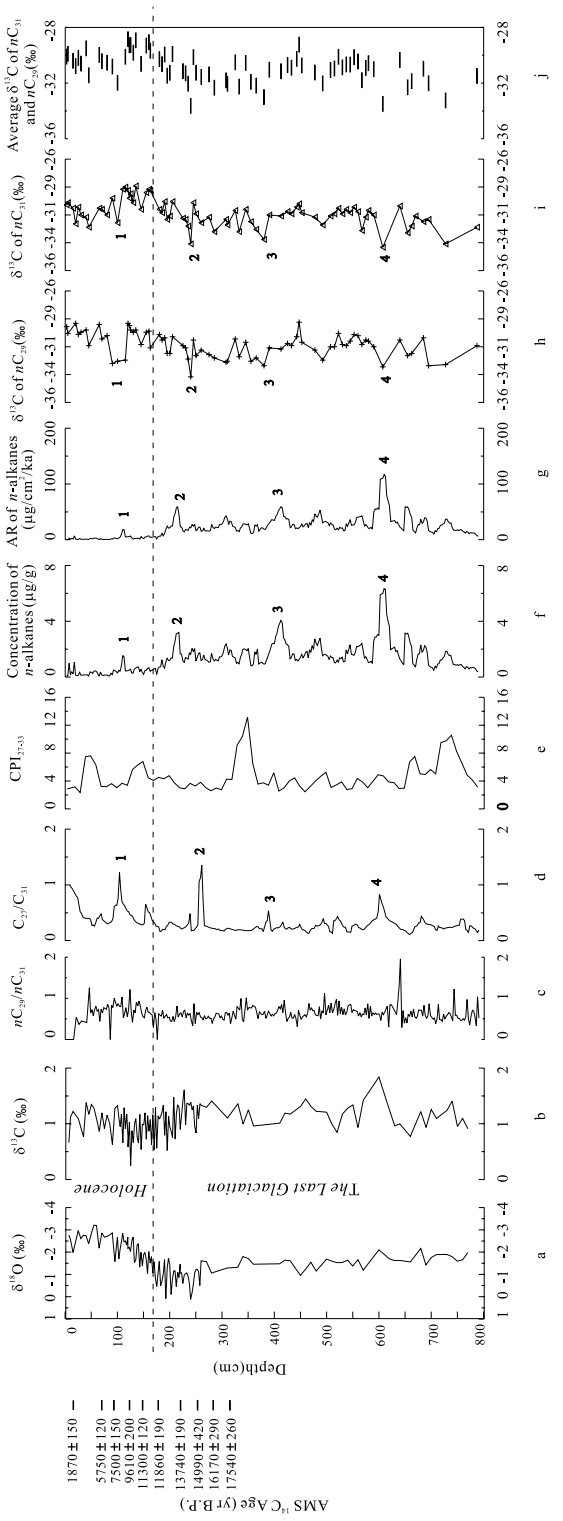

Fig. 4. Depth profiles of the geochemical data from Core 17962. (a) $\delta^{18}O$ of planktonic foraminifera *Globigerinoides sacculifer* (Fang, personal communication, 2001). (b) $\delta^{13}C$ of planktonic foraminifera *G. sacculifer* (Fang, personal communication, 2001). (c) Relative ratio of *n*-C_{29} alkane to *n*-C_{31} alkane at *m/z* 85. (d) Relative ratio of *n*-C_{27} alkane to *n*-C_{31} alkane at *m/z* 85. (e) CPI_{27-33}. (f) Concentration of *n*-alkanes from C_{27} to C_{33}. (g) AR, accumulation rate of *n*-alkanes from C_{27} to C_{31} (when calculating the accumulation rates, the sedimentation rates below 309.25 cm are the same as at the depth of 309.25 cm). (h) $\delta^{13}C$ of C_{29} *n*-alkanes. (i) $\delta^{13}C$ of C_{31} *n*-alkanes. (j) Weighted average $\delta^{13}C$ of *n*-C_{31} and *n*-C_{29}. The numbers (1, 2, 3 and 4) mark the peaks of *n*-alkanes C_{27}/C_{31}, concentration of *n*-alkanes and AR of *n*-alkanes, and excursions of $\delta^{13}C$ of *n*-C_{29} and *n*-C_{31}.

3. Results and discussion

3.1. Distribution of n-alkanes

Mass chromatograms *m/z* 85 for *n*-alkane fractions of sediments are shown in Fig. 3. A unimodal distribution of *n*-alkanes is observed in all sediment samples, maximizing at C_{31}. The total concentrations of the odd-carbon-numbered C_{27} to C_{33} *n*-alkanes extracted from Core 17962 are presented in Fig. 4. The carbon preference indices (CPI; $CPI_{27-33} = 0.5\Sigma C_{27,29,31,33}(1/\Sigma C_{26,28,30,32}+1/\Sigma C_{28,30,32,34})$) for *n*-alkanes in the range C_{27}–C_{33} vary from 2.45 to 13.17 (Fig. 4 and Appendix), indicating a pronounced odd-carbon predominance. The predominance of the odd-carbon-numbered *n*-C_{27} to *n*-C_{33} homologs is characteristic of the *n*-alkanes derived from terrestrial plant epicuticular leaf waxes (Eglinton and Hamilton, 1967; Collister et al., 1994), thus suggesting a terrigenous higher plant origin for the long-chain *n*-alkanes.

Noticeably, the CPIs are very high (up to 13.17) at the depth of 327.5–357.5 cm, which may reflect that the sedimentary environments were very oxic and fatty acids and fatty alcohols in the sediments were oxidized to odd-carbon-numbered *n*-alkanes. However, more evidence is needed to support this interpretation.

Terrestrial material in the studied area can be transported into marine sediments by two primary ways: water and wind/dust. Intuitively, dust inputs are more important under windy and arid

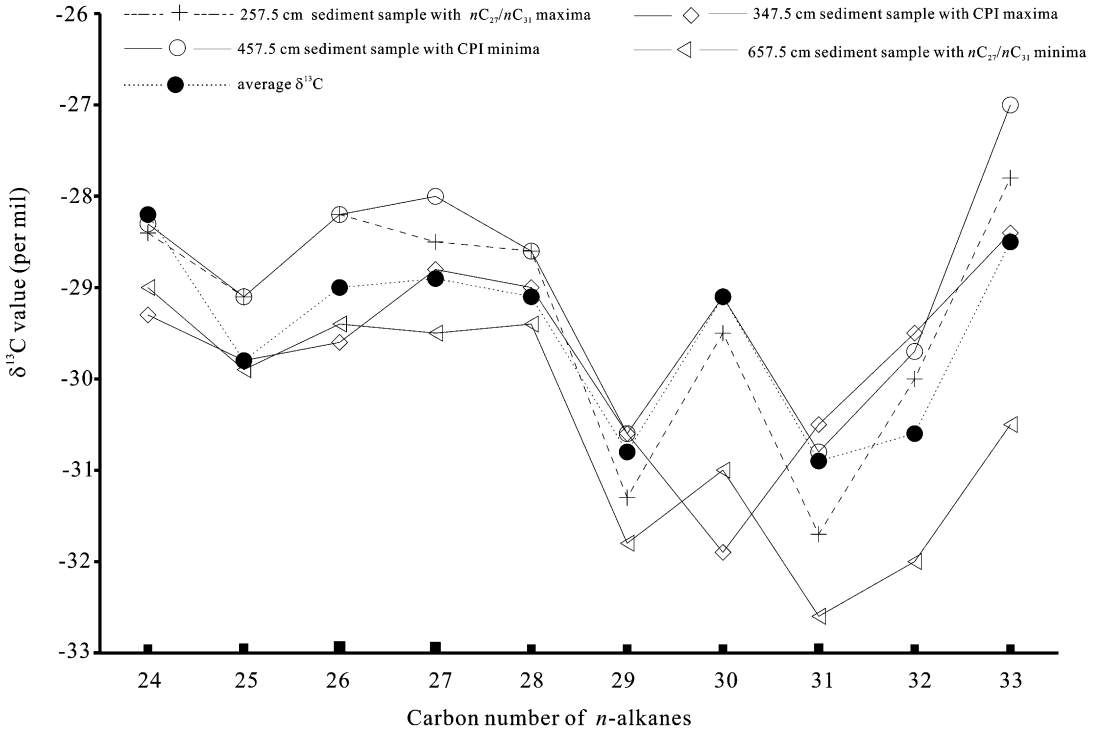

Fig. 5. Distribution of the $\delta^{13}C$ values of C_{24}–C_{33} *n*-alkanes and average $\delta^{13}C$ for *n*-C_{29} and *n*-C_{31} alkanes. The samples were selected to display the extremes of distributions viz. low and high CPI and high and low C_{27}/C_{31}.

conditions, while river-borne particles might contribute more significantly during more humid periods (Zhao et al., 2000). In the southern SCS, as evidenced by the grain-size distribution, the terrestrial input contribution was mainly from river-borne sediments. In particular, at two neighboring sites, 17961 and 17964 (Fig. 1), fluvial clays amount to 97–98% and 93–95%, respectively, during the glaciation. They tend to decrease to 96% at Site 17961 and to 88–91% at Site 17964 in the Holocene (Wang et al., 1999). Core 17962, which is located between Cores 17961 and 17964, must have similar variation of river-borne clay contents and thus a parallel contribution.

The accumulation rates and concentrations of long-chain *n*-alkanes (C_{27}–C_{33}) show a general glacial/interglacial trend. They were higher in the last glacial period than in the Holocene and fluctuated greatly during the last glacial period (Fig. 4f,g and Appendix). The SCS has experienced major changes in sea level (i.e. position of the coastline) during glacial time (Hanebuth et al., 2000). The Molengraaff River developed in the southern emergent tropical lowland and debouched near Site 17962 during the last glacial period of low sea level (Fig. 1). Thus, long-chain *n*-alkanes derived from terrestrial plants of Core 17962 are likely to reflect the flux changes of the materials transported by the river which, in turn, would have been influenced by sea level and precipitation. The lower the sea level and the higher the precipitation, the higher the accumulation rates and concentrations of long-chain *n*-alkanes (C_{27}–C_{33}).

In addition to the general glacial/interglacial trend, the accumulation rate of long-chain *n*-alkanes shows some specific features; in particular, it is extremely high near the depth of 620 cm (Fig. 4g), corresponding to a decrease in sea-surface salinity (SSS) of Core 17961 as estimated by the $\delta^{18}O$ values of the planktonic foraminifera *Globigerinoides ruber* (Wang et al., 1999). This

increase is ascribed to higher contributions of terrigenous organic matter as a result of higher precipitation (Pelejero et al., 1999a).

3.2. Carbon-isotopic composition of long-chain n-alkanes

Stable carbon isotopes were determined for individual C_{24}–C_{33} *n*-alkanes (Fig. 5). Downcore $\delta^{13}C$ profiles of the individual odd-carbon-numbered C_{29} and C_{31} *n*-alkanes shown in Fig. 4h,i do not depict any systematic glacial/interglacial trend. The $\delta^{13}C$ value for *n*-C_{31} alkane is close to that of *n*-C_{29} alkane, indicating their common biosynthetic origin (Collister et al., 1994; Bird et al., 1995).

The $\delta^{13}C$ values of *n*-alkanes extracted from modern C_3 and C_4 plants are within the range of −28‰ to −43‰ and −20‰ to −26‰ (Rieley et al., 1991; Collister et al., 1994). In Core 17962, the $\delta^{13}C$ values of C_{27} to C_{31} *n*-alkanes vary from −27.1‰ to −33.9‰, falling within the range of corresponding *n*-alkanes in modern leaves mainly from C_3 land plants (Freeman and Colarusso, 2001). The isotopic values of plant wax *n*-alkanes are related not only to the photosynthetic mechanisms, but also to the $\delta^{13}C$ of atmospheric CO_2 and the physiological responses of the plants to the environmental conditions (Zhao et al., 2000). For example, a lower concentration of atmospheric CO_2 could lead to the reduction of fractionation of stable carbon isotope, explaining the increase by about 1‰ on $\delta^{13}C$ values of tree leaf cellulose in the last glacial period (Zhao et al., 2000). However, changes in the concentration and $\delta^{13}C$ of atmospheric CO_2 over the last 35 kyr (Leuenberger et al., 1992) are unlikely to have had major effects on the $\delta^{13}C$ of the leaf wax *n*-alkanes. So the $\delta^{13}C$ values (−27.1‰ to −33.9‰) of *n*-alkanes in the sediments from Core 17962 reflect that they mainly derived from C_3 higher plants.

At the same time, no variation in $\delta^{13}C$ values of *n*-alkanes along the whole core sequence suggests that C_3-type vegetation prevailed in the southern coastal areas of the southern SCS during the Holocene and in the emerged Sunda Land during the Last Glacial Stage. Pollen records of Core 17964 revealed that two alternative ecological groups were predominating on Sunda Land or along the southern coastal areas of the southern SCS during the glacial–Holocene cycle. The first group includes tropical montane rainforest gymnosperms (*Podocarpus*, *Dacrycarpus*, *Dacrydium* and *Phyllocladus*), indicating a cool and humid climate, and the second group is dominated by tropical lowland rainforest taxa, including *Altingia*, *Alchornea*, *Mallotus* and mangroves, reflecting a hot and humid climate (Sun et al., 2000).

However, as shown in Fig. 4h,i, the $\delta^{13}C$ values of *n*-alkanes were much lower at episodes 1, 2, 3 and 4, which possibly represent short phases of increased humidity (Sukumar et al., 1993). It is interesting to note that the excursions 1–4 correspond well with the peaks in C_{27} *n*-alkane/C_{31} *n*-alkane ratio (Fig. 4d), and the concentrations and accumulation rates of long-chain *n*-alkanes (Fig. 4f,g). Brincat et al. (2000) suggested that variations in C_{27} *n*-alkane/C_{31} *n*-alkane ratio with depth might reflect a change in the subtype of vegetation in the hinterland. Therefore, the distribution of the $\delta^{13}C$ values of *n*-alkanes and the peaks of C_{27} *n*-alkane/C_{31} *n*-alkane ratio in the sediments from Core 17962 possibly suggest that C_3 plants dominated the paleovegetation on Sunda Land during the glaciation, but the subtypes of vegetation possibly changed when the moisture was enhanced.

As indicated in Fig. 5, the $\delta^{13}C$ values are relatively uniform for C_{24} to C_{28} *n*-alkanes along the depth profile. But for C_{28} to C_{33} *n*-alkanes, the even-carbon-numbered *n*-alkanes are isotopically heavier than the co-occurring odd-numbered *n*-alkanes, which are similar in isotopic composition to *n*-alkanes in offshore New Zealand sediments (Kennicutt and Brooks, 1990). It is easily thought that the odd and even *n*-alkanes are of independent bio-origins (Kennicutt and Brooks, 1990). However, the $\delta^{13}C$ values of *n*-alkane homologs from the waxes of a single plant can vary up to 6‰ (averaged at 2.4‰), which may be the result of production of different leaf wax lipids in different proportions during a leaf's growth cycle (Collister et al., 1994). It may also be possible that the odd and even *n*-alkanes were biosynthe-

sized by different biosynthetic pathways. At present, it is uncertain which interpretation is more reasonable.

3.3. Humidity on the Sunda Shelf

As viewed from the studies of molecular distribution and carbon-isotopic composition of *n*-alkanes extracted from hemipelagic sediments in the southern SCS, terrestrial input was enhanced during the last glacial. The $\delta^{13}C$ values, spanning the last glacial period, for long-chain *n*-alkanes show no systematic glacial/interglacial trend. Moreover, the carbon-isotopic composition of *n*-alkanes indicates their main C_3 higher plant origin. Therefore, the vegetation covering the Southern Shelf experienced no obvious change; the climate on Sunda Land will not have been drier during the last glacial period as compared to the present.

At the same time, pollen records reflect that rainforest floras existed in SE Asia and northern Australia during the last glacial period (Grindrod et al., 2002), and tropical rainforests are a feature of the most humid environment. Therefore, the climate in the north Australian and Indonesian continental shelf and oceans was humid during the last glaciation.

The Asian monsoon system may have contributed considerably to the precipitation on the emerged continental shelf of the SCS (Wang, 1999). The reduction of sea area and the drop of SST during the glacial period in the West Pacific marginal seas (Wang, 1999) resulted in a decrease in evaporation rate from the sea, while the weakened summer monsoon would have brought less precipitation to the East Asian land, thus intensifying aridity during the Last Glacial Maximum (LGM) (Wang et al., 1997). These factors explain the intense aridity on the northern shelf of the SCS as reconstructed from pollen studies (Sun et al., 2000; Fig. 1). By contrast, the climate on the Sunda Shelf was humid in the last glacial period, because during that time the strengthened winter monsoon absorbed enough moisture when crossing the SCS and transferred more vapor to the emerged Southern Shelf of the SCS (Sun et al., 2000).

4. Conclusions

The *n*-alkanes extracted from the sediments of Core 17962 show the predominance of odd-carbon-numbered alkanes in the C_{27} to C_{33} range, consistent with a terrestrial plant epicuticular wax origin. Moreover, the downcore isotopes of *n*-alkanes display almost no change, suggesting the vegetation has experienced little change on the Sunda Shelf since the last glaciation.

The accumulation rate of long-chain *n*-alkanes (C_{27}–C_{33}) in the sediments from Core 17962 in the last glacial period was high as compared to that during the Holocene, and increased sharply near the depth of 620 cm. These depth profiles are generally consistent with previous records based on the $\delta^{18}O$ and $\delta^{13}C$ values of planktonic foraminifera *Globigerinoides ruber* and SSS analyses of Cores 17964 and 17961, suggesting that intensified river flows occurred on Sunda Land due to intensification of winter monsoon precipitation during the last glacial period of low sea level.

Compound-specific isotopic analyses revealed no systematic glacial/interglacial shift of $\delta^{13}C$ values. The isotopic composition ranges from $-27.1‰$ to $-33.9‰$ for C_{27}–C_{33} *n*-alkanes in the entire core sequence, indicating an input mainly from C_3 higher plants, which is consistent with previous pollen studies that tropical rainforest and mangroves dominated on the Sunda Shelf (Sun et al., 2000). This glacial vegetation could be the result of enhanced winter monsoon that led to more precipitation on the Southern Shelf and provided the Sunda Land with a humid climate.

Acknowledgements

The authors wish to thank Dr. Chao Li at the State Key Laboratory of Organic Geochemistry, CAS for his assistance in GC/IR/MS operation. They also thank Dr. De Deckker and Carles Pelejero and Prof. G. Eglinton and M. Sarnthein for critical review of earlier drafts of the manuscript. This project was granted by the National Natural Science Foundation of China (Grant No. 49453004) and the State Key Basic Research Special Foundation (No. G2000078500).

Appendix

Sample depth, TOC, total concentration of long-chain *n*-alkanes, the carbon number range of long-chain *n*-alkanes (C-range), the maximal carbon number of long-chain *n*-alkanes (C_{max}), CPI_{27-33}, $nC_{27}/n\ C_{31}$, $\delta^{13}C_{29}$ and $\delta^{13}C_{31}$ of the studied sediments.

Depth (cm)	TOC (%)[a]	Total L-*n*-alkane[b]	C-range	C_{max}	CPI_{27-33}[c]	*n*-C_{27}/*n*-C_{31}	$\delta^{13}C_{29}$ (‰)	$\delta^{13}C_{31}$ (‰)
2.5	0.714	0.968	C_{23}–C_{31}	C_{31}	2.84	0.99	−29.2	−30.1
17.5	0.603	1.032	C_{24}–C_{33}	C_{33}	3.17	0.93	−28.9	−31.8
27.5	0.674	0.328	C_{24}–C_{31}	C_{31}	2.32	0.52	−29.8	−30.5
37.5	0.585	0.159	C_{22}–C_{31}	C_{31}	7.48	0.40	−29.6	−31.1
47.5	0.676	0.353	C_{23}–C_{33}	C_{33}	7.60	0.38	−30.9	−32.1
57.5	0.697	0.429	C_{22}–C_{33}	C_{33}	6.29	0.33	–	–
67.5	0.570	0.351	C_{22}–C_{31}	C_{31}	3.23	0.48	−29.0	−30.4
77.5	0.650	0.131	C_{21}–C_{31}	C_{31}	3.18	0.32	−30.1	−30.7
87.5	0.562	0.267	C_{21}–C_{31}	C_{31}	3.62	0.34	−32.5	−30.3
97.5	0.662	0.408	C_{22}–C_{33}	C_{31}	3.02	0.63	−32.1	−31.2
107.5	0.637	0.812	C_{22}–C_{33}	C_{31}	3.69	0.70	−31.3	−28.7
117.5	0.558	0.438	C_{24}–C_{31}	C_{31}	3.39	0.53	−32.2	−28.5
127.5	0.618	0.272	C_{24}–C_{33}	C_{33}	5.64	0.44	−29.6	−29.4
137.5	0.615	0.703	C_{22}–C_{31}	C_{31}	6.30	0.31	−29.5	−28.4
147.5	0.705	0.301	C_{22}–C_{33}	C_{31}	6.78	0.28	−30.8	−30.5
157.5	0.783	0.614	C_{23}–C_{31}	C_{31}	4.46	0.51	−29.6	−28.5
167.5	0.757	0.521	C_{22}–C_{33}	C_{31}	4.08	0.33	−31.1	−28.8
177.5	0.863	0.615	C_{24}–C_{31}	C_{31}	4.52	0.24	−29.9	−30.5
187.5	0.636	0750	C_{24}–C_{33}	C_{31}	4.33	0.20	−30.3	−30.3
197.5	0.653	1.169	C_{23}–C_{33}	C_{31}	4.76	0.32	−31.6	−31.2
207.5	0.851	2.189	C_{22}–C_{33}	C_{31}	3.77	0.29	−30.1	−29.8
217.5	0.682	3.200	C_{24}–C_{33}	C_{33}	3.01	0.24	–	–
227.5	0.726	1.048	C_{24}–C_{34}	C_{33}	2.87	0.23	−31.0	−31.3
237.5	0.771	1.721	C_{24}–C_{32}	C_{31}	3.66	0.48	−32.9	−32.8
247.5	0.729	2.021	C_{24}–C_{33}	C_{33}	3.28	0.21	−31.1	−30.4
257.5	0.730	1.731	C_{21}–C_{33}	C_{31}	3.83	1.13	−31.3	−31.7
267.5	0.709	1.228	C_{22}–C_{33}	C_{31}	3.05	0.26	−31.7	−31.2
277.5	0.680	1.081	C_{26}–C_{33}	C_{31}	2.58	0.23	−31.4	−31.3
287.5	0.760	1.251	C_{22}–C_{33}	C_{31}	2.97	0.20	−32.0	−32.5
297.5	0.683	1.439	C_{22}–C_{33}	C_{31}	2.74	0.18	–	–
307.5	0.650	2.378	C_{22}–C_{33}	C_{31}	4.26	0.21	−32.4	−31.4
317.5	0.790	1.908	C_{23}–C_{33}	C_{31}	4.22	0.33	−32.3	−31.9
327.5	0.712	0.987	C_{23}–C_{33}	C_{33}	9.14	0.35	−30.3	−30.6
337.5	0.701	1.646	C_{24}–C_{32}	C_{31}	10.40	0.66	−31.9	−32.5
347.5	0.672	1.888	C_{22}–C_{33}	C_{31}	13.17	0.34	−30.6	−30.5
357.5	0.651	0.793	C_{25}–C_{33}	C_{31}	6.48	0.17	−32.3	−31.6
367.5	0.755	2.013	C_{23}–C_{33}	C_{31}	3.56	0.25	−32.0	−32.3
377.5	0.654	0.988	C_{23}–C_{33}	C_{31}	3.75	0.16	−31.9	−33.2
387.5	0.795	1.462	C_{24}–C_{33}	C_{31}	3.40	0.19	−31.1	−31.0
397.5	0.637	2.418	C_{22}–C_{33}	C_{33}	5.18	0.21	–	–
407.5	0.714	3.621	C_{22}–C_{33}	C_{33}	2.54	0.23	−31.1	−31.0
417.5	0.731	2.809	C_{22}–C_{33}	C_{31}	3.02	0.24	−31.2	−31.1
427.5	0.829	2.161	C_{23}–C_{33}	C_{33}	4.03	0.24	−30.7	−30.7
437.5	0.733	1.652	C_{23}–C_{33}	C_{31}	4.45	0.22	−30.9	−30.9
447.5	0.595	–	C_{23}–C_{34}	C_{31}	3.26	0.29	−28.8	−30.0
457.5	0.680	1.518	C_{21}–C_{34}	C_{31}	2.45	0.18	−30.6	−30.8
467.5	0.716	1.948	C_{24}–C_{33}	C_{31}	3.21	0.18	−30.9	−30.5
477.5	0.635	2.732	C_{24}–C_{33}	C_{31}	4.01	0.27	−31.3	−31.2
487.5	0.709	2.787	C_{22}–C_{33}	C_{31}	4.66	0.29	−31.7	−31.5

Appendix (*continued*).

Depth (cm)	TOC (%)[a]	Total L-*n*-alkane[b]	C-range	C_{max}	CPI_{27-33}[c]	*n*-C_{27}/*n*-C_{31}	$\delta^{13}C_{29}$ (‰)	$\delta^{13}C_{31}$ (‰)
497.5	0.634	1.627	C_{24}–C_{33}	C_{31}	5.27	0.31	−32.2	−31.9
507.5	0.586	1.504	C_{24}–C_{33}	C_{31}	3.07	0.16	−31.0	−31.1
517.5	0.637	1.010	C_{24}–C_{33}	C_{31}	3.44	0.39	−31.0	−30.9
527.5	0.631	1.321	C_{24}–C_{33}	C_{31}	3.89	0.31	−30.8	−30.6
537.5	0.661	1.946	C_{22}–C_{33}	C_{31}	2.76	0.16	−30.9	−30.5
547.5	0.675	1.611	C_{24}–C_{32}	C_{31}	2.89	0.26	−30.5	−30.8
557.5	0.661	2.198	C_{24}–C_{33}	C_{31}	4.36	0.28	−30.0	−30.7
567.5	0.631	2.405	C_{24}–C_{33}	C_{31}	3.86	0.19	−30.8	−32.4
577.5	0.630	1.264	C_{24}–C_{33}	C_{31}	3.02	0.27	−30.4	−31.2
587.5	0.625	0.972	C_{22}–C_{35}	C_{33}	3.96	0.36	−31.0	−31.0
597.5	0.679	3.023	C_{22}–C_{35}	C_{31}	4.90	0.52	–	–
607.5	0.750	6.007	C_{22}–C_{33}	C_{31}	4.73	0.60	−32.8	−33.9
617.5	0.711	4.029	C_{22}–C_{33}	C_{31}	3.86	0.37	–	–
627.5	0.656	–	C_{22}–C_{33}	C_{31}	3.79	0.32	–	–
637.5	0.661	1.569	C_{26}–C_{33}	C_{33}	2.90	0.23	−30.4	−30.2
647.5	0.569	0.880	C_{22}–C_{35}	C_{31}	2.96	0.19	−31.1	−31.4
657.5	0.644	2.878	C_{20}–C_{33}	C_{31}	6.74	0.11	−31.8	−32.6
667.5	0.574	0.859	C_{22}–C_{35}	C_{31}	7.53	0.24	−31.0	−31.1
677.5	0.615	1.671	C_{22}–C_{35}	C_{33}	5.03	0.32	–	–
687.5	0.583	2.248	C_{23}–C_{33}	C_{31}	4.95	0.31	−30.2	−31.6
697.5	0.586	0.742	C_{22}–C_{33}	C_{31}	5.65	0.29	−32.7	−31.4
707.5	0.583	0.769	C_{24}–C_{33}	C_{33}	5.03	0.19	–	–
717.5	0.586	1.223	C_{22}–C_{33}	C_{31}	9.53	0.23	–	–
727.5	0.538	1.816	C_{22}–C_{33}	C_{33}	9.76	0.22	−32.6	−33.6
737.5	–	1.556	C_{24}–C_{33}	C_{33}	10.58	0.24	–	–
747.5	0.656	0.848	C_{22}–C_{33}	C_{33}	8.24	0.27	–	–
757.5	–	0.896	C_{24}–C_{33}	C_{31}	6.56	0.39	–	–
767.5	0.557	0.749	C_{22}–C_{33}	C_{33}	4.87	0.18	–	–
777.5	0.609	0.661	C_{22}–C_{35}	C_{33}	4.15	0.24	–	–
787.5	0.574	0.401	C_{26}–C_{33}	C_{31}	3.14	0.14	−30.9	−32.1

[a] TOC data from Jia et al. (2002).

[b] Total L-*n*-alkanes = ΣC_{27-33} and the concentration expressed as μg/g dry sediments.

[c] $CPI_{27-33} = 0.5\Sigma C_{27,29,31,33}(1/\Sigma C_{26,28,30,32}+1/\Sigma C_{28,30,32,34})$.

References

Bird, M.I., Summons, R.E., Gagan, M.K., Roksandic, Z., Dowling, L., Head, J., Fifield, L.K., Cresswell, R.G., Johnson, D.P., 1995. Terrestrial vegetation changes inferred from *n*-alkanes $\delta^{13}C$ analysis in the marine environment. Geochim. Cosmochim. Acta 59, 2853–2857.

Brincat, D., Yamada, K., Ishiwatari, R., Uemura, H., Naraoka, H., 2000. Molecular-isotopic stratigraphy of long-chain *n*-alkanes in Lake Baikal Holocene and glacial age sediments. Org. Geochem. 31, 287–294.

Broecker, W.S., Andree, M., Klas, M. et al., 1988. New evidence from the South China Sea for an abrupt termination of the glacial period. Nature 333, 156–158.

Collister, J.W., Rieley, G., Stern, B., Eglinton, G., Fry, B., 1994. Compound-specific $\delta^{13}C$ analyses of leaf lipids from plants with differing carbon dioxide metabolisms. Org. Geochem. 21, 619–627.

Eglinton, G., Hamilton, R.J., 1967. Leaf epicuticular waxes. Science 156, 1322–1335.

Freeman, K.H., Colarusso, L.A., 2001. Molecular and isotopic records of C4 grassland expansion in the late Miocene. Geochim. Cosmochim. Acta 65, 1439–1454.

Grindrod, J., Moss, P., van der Kaars, S., 2002. Late Quaternary mangrove pollen records from continental shelf and ocean cores in the North Australian-Indonesian region. In: Kershaw, P., David, B., Tapper, N., Penny, D., Brown, J. (Eds.), Bridging Wallace's Line: The Environmental and Cultural History and Dynamics of the SE-Asian-Australian Region (Advances in GeoEcology 34). Catena Verlag, Reiskirchen, pp. 119–146.

Gupta, A., Rahman, A., Wong, P.P., Pitts, J., 1987. The Old Alluvium of Singapore and the extinct drainage system to the South China Sea. Earth Surf. Process. Landforms 12, 259–275.

Hanebuth, T., Stattegger, K., Grootes, P.M., 2000. Rapid

flooding of the Sunda Shelf: A Late-Glacial sea level record. Science 288, 1033–1035.

Huang, Y., Dupont, L., Sarnthein, M., Hayes, J.M., Eglinton, G., 2000. Mapping of C_4 plant input from North West Africa into North East Atlantic sediments. Geochim. Cosmochim. Acta 64, 3505–3513.

Huang, Y., Lockheart, M.J., Collister, J.W., Eglinton, G., 1995. Molecular and isotopic biogeochemistry of the Miocene Clarkia Formation: hydrocarbons and alcohols. Org. Geochem. 23, 785–801.

Huang, Y., Street-Perrott, F.A., Metcalfe, S.E., Brenner, M., Moreland, M., Freeman, K.H., 2001. Climate change as the dominant control on glacial-interglacial variations in C_3 and C_4 plant abundance. Science 291, 1647–1651.

Jia, G., Peng, P., Fang, D., 2002. Burial of different types of organic carbon in Core 17962 from South China Sea since the last glacial period. Quat. Res. 58, 93–100.

Kennicutt, M.C., II, Brooks, J.M., 1990. Unusual normal alkane distributions in offshore New Zealand sediments. Org. Geochem. 15, 193–197.

Kershaw, P., van der Kaars, S., Moss, P., Wang, S., 2002. Quaternary records of vegetation, biomass burning, climate and possible human impact in the Indonesian-Northern Australian region. In: Kershaw, P., David, B., Tapper, N., Penny, D., Brown, J. (Eds.), Bridging Wallace's Line: The Environmental and Cultural History and Dynamics of the SE-Asian-Australian Region (Advances in GeoEcology 34). Catena Verlag, Reiskirchen, pp. 97–118.

Kuypers, M.M.M., Pancost, R.D., Sinninghe Damste, J.S., 1999. A large and abrupt fall in atmospheric CO_2 concentration during Cretaceous times. Nature 399, 342–345.

Leuenberger, M., Siegenthaler, U., Langway, C.C., 1992. Carbon isotope composition of atmospheric CO_2 during the last ice age from an Antarctic ice core. Nature 357, 488–490.

Molengraaff, G.A.F., 1921. Modern deep-sea research in the East Indian Archipelago. Geogr. J. 57, 95–121.

Pagani, M., Freeman, K.H., Arthur, M.A., 1999. Late Miocene atmospheric CO_2 concentrations and the expansion of C4 grasses. Science 285, 876–879.

Pelejero, C., Grimalt, J.O., Sarnthein, M., Wang, L., Flores, J.A., 1999a. Molecular biomarker record of sea surface temperature and climatic change in the South China Sea during the last 140,000 years. Mar. Geol. 156, 109–121.

Pelejero, C., Kienast, M., Wang, L., Grimalt, J.O., 1999b. The flooding of Sundaland during the last deglaciation: imprints in hemipelagic sediments from the southern South China Sea. Earth Planet. Sci. Lett. 171, 661–671.

Rieley, G., Collier, R.J., Jones, D.M., Eglinton, G., Eakin, P.A., Fallick, E., 1991. Sources of sedimentary lipids deduced from stable carbon-isotope analyses of individual compounds. Nature 352, 425–427.

Sarnthein, M., Pflaumann, U., Wang, P., Wong, H.K. (Eds.), 1994. Preliminary Report on Sonne-95 Cruise 'Monitor Monsoon' to the South China Sea. Ber. Rep., Geol.-Paläontol. Inst. Univ. Kiel 68, 11–25.

Smith, B.N., Epstein, S., 1971. Two categories of $^{13}C/^{12}C$ ratios for higher plants. Plant Physiol. 47, 380–384.

Sukumar, R., Ramesh, R., Pant, R.K., Rajagopalan, G., 1993. A $\delta^{13}C$ record of late Quaternary climate change from tropical peats in southern India. Nature 364, 703–706.

Sun, X., Li, X., 1999. A pollen record of the last 37 ka in deep sea core 17940 from the northern slope of the South China Sea. Mar. Geol. 156, 227–244.

Sun, X., Li, X., Luo, Y., Chen, X., 2000. The vegetation and climate at the last glaciation on the emerged continental shelf of the South China Sea. Paleogeogr. Paleoclimatol. Paleoecol. 160, 301–316.

van der Kaars, S., Wang, X., Kershaw, P., Guichard, F., Setiabudi, D.A., 2000. A Late Quaternary palaeoecological record from the Banda Sea, Indonesia: patterns of vegetation, climate and biomass burning in Indonesia and northern Australia. Paleogeogr. Paleoclimatol. Paleoecol. 155, 135–153.

Wang, L., Sarnthein, M., Erlenkeuser, H., Grimalt, J., Grootes, P., Heilig, S., Ivanova, E., Kienast, M., Pelejero, C., Pflaumann, U., 1999. East Asian monsoon climate during the Late Pleistocene: high-resolution sediment records from the South China Sea. Mar. Geol. 156, 245–284.

Wang, L., Wang, P., 1990. Late Quaternary paleoceanography of the South China Sea: glacial-interglacial contrast in an enclosed basin. Paleoceanography 5, 77–90.

Wang, P., 1999. Response of Western Pacific marginal seas to glacial cycles: Paleoceanography and sedimentological features. Mar. Geol. 156, 5–39.

Wang, P., Bradshaw, M., Ganzei, S.S., Tsukawaki, S., Hassan, K.B., Hantoro, W.S., Poobrasert S., Burne, R., Zhao, Q., Kagami, H., 1997. West Pacific Marginal Seas during the Last Glacial Maximum: amplification of environmental signals and its impact on monsoon climate. Proc. 30th Int. Geol. Congr. 13. VSP, Utrecht, pp. 65–86.

Zhao, M., Eglinton, G., Haslett, S.K., Jordan, R.W., Sarnthein, M., Zhang, Z., 2000. Marine and terrestrial biomarker records for the last 35,000 years at ODP site 658C off NW Africa. Org. Geochem. 31, 919–930.